

On the first Sonine correction for granular gases

François Coppex,¹ Michel Droz,¹ Jarosław Piasecki,² and Emmanuel Trizac³

¹*Department of Physics, University of Genève, CH-1211 Genève 4, Switzerland*

²*Institute of Theoretical Physics, University of Warsaw, PL-00 681 Warsaw, Poland*

³*Laboratoire de Physique Théorique (UMR 8627 du Cnrs),
Bâtiment 210, Université de Paris-Sud, 91405 Orsay, France*

We consider the velocity distribution for a granular gas of inelastic hard spheres described by the Boltzmann equation. We investigate both the free of forcing case and a system heated by a stochastic force. We propose a new method to compute the first correction to Gaussian behavior in a Sonine polynomial expansion quantified by the fourth cumulant a_2 . Our expressions are compared to previous results and to those obtained through the numerical solution of the Boltzmann equation. It is numerically shown that our method yields very accurate results for small velocities of the rescaled distribution. We finally discuss the ambiguities inherent to a linear approximation method in a_2 .

Most theories of rapid granular flows consider a granular gas as an assembly of inelastic hard spheres and assume uncorrelated binary collisions described by the Boltzmann equation, with a possible Enskog correction to account for excluded volume effects [1, 2, 3, 4, 5, 6, 7, 8, 9, 10, 11, 12]. The deviations from the Maxwellian velocity distribution may be accounted for by an expansion in Sonine polynomials, and it is often sufficient to retain only the leading term in this expansion, quantified by a_2 , the fourth cumulant of the velocity distribution [2, 5, 8, 13, 14]. The purpose of this paper is twofold: first, we present a novel route to compute a_2 , directly inspired from a method that has been recently proposed to compute with accuracy the decay exponents and non Maxwellian features of gas subjected to ballistic annihilation dynamics [15, 16] (where particles undergoing free flight motion disappear upon contact [17, 18]). In essence, this method considers the limit of vanishing velocities of the Boltzmann equation, and deduces a_2 from moments of the velocity distribution that are *a priori* of lower order than those involved in the standard derivation [4, 8]. We may consequently expect a better precision from this alternative approach, that is analytically simpler to work out. We also know that the velocity distribution is non Gaussian at high energies [4, 8], so that extracting the relevant kinetic information from the behavior at vanishing velocities seems a promising route. The second goal of this article is to discuss the ambiguities –common to both approaches– encountered performing computations up to linear order in a_2 , neglecting not only higher order Sonine contributions but also terms in a_2^k , $k = 2, 3$. Such an ambiguity has first been mentioned by Montanero and Santos [8].

Within the framework of the Boltzmann equation, the one-particle velocity distribution function $f(\mathbf{v}; t)$ for a homogeneous system free of forcing obeys the relation

$$\partial_t f(\mathbf{v}_1; t) = I(f, f), \quad (1)$$

where the collision integral reads

$$I(f, f) = \sigma^{d-1} \int_{\mathbb{R}^d} d\mathbf{v}_2 \int d\hat{\boldsymbol{\sigma}} \theta(\hat{\boldsymbol{\sigma}} \cdot \hat{\mathbf{v}}_{12}) (\hat{\boldsymbol{\sigma}} \cdot \mathbf{v}_{12}) \left[\frac{1}{\alpha^2} f(\mathbf{v}_1^{**}; t) f(\mathbf{v}_2^{**}; t) - f(\mathbf{v}_1; t) f(\mathbf{v}_2; t) \right]. \quad (2)$$

In Eq. (2), σ is the diameter of the particles, θ the Heaviside distribution, $\mathbf{v}_{12} = \mathbf{v}_1 - \mathbf{v}_2$ the relative velocity of two particles, $\hat{\mathbf{v}}_{12} = \mathbf{v}_{12}/v_{12}$, $v_{12} = |\mathbf{v}_{12}|$, and $\hat{\boldsymbol{\sigma}}$ a unit vector joining the centers of the grains. The space dimension is d . The precollisional velocities \mathbf{v}_i^{**} and the postcollisional ones \mathbf{v}_i are related by

$$\mathbf{v}_1^{**} = \mathbf{v}_1 - \frac{1 + \alpha}{2\alpha} (\mathbf{v}_{12} \cdot \hat{\boldsymbol{\sigma}}) \hat{\boldsymbol{\sigma}}, \quad (3a)$$

$$\mathbf{v}_2^{**} = \mathbf{v}_2 + \frac{1 + \alpha}{2\alpha} (\mathbf{v}_{12} \cdot \hat{\boldsymbol{\sigma}}) \hat{\boldsymbol{\sigma}}, \quad (3b)$$

with $\alpha \in [0, 1]$ the restitution coefficient. If energy is supplied to the system, an additional forcing term is present in Eq. (1) [8], but the general arguments and method presented below remain valid. To be more specific, we shall also consider the situation where the system is driven into a non equilibrium steady state by a random force acting on the particles [4, 6, 8]. With this energy feeding mechanism, coined “stochastic thermostat”, the Fokker-Planck term $\xi_0^2 \nabla_{\mathbf{v}}^2 f$ should be added to the right-hand side (r.h.s.) of Eq. (1) [4], where ξ_0 is related to the amplitude of the random force acting on the grains.

We are searching for an isotropic scaling solution $\tilde{f}(c)$ of Eq. (2). The requirement of a time independent behavior with respect to the typical velocity $v_0(t) = \sqrt{2\langle \mathbf{v}^2 \rangle / d}$ imposes that [2, 4, 8]

$$f(\mathbf{v}; t) = \frac{n}{v_0^d(t)} \tilde{f}(c), \quad (4)$$

where the rescaled velocity is given by $c = v/v_0(t)$ and the angular brackets $\langle \cdot \rangle$ denote the average over $f(\mathbf{v}; t)$. The presence of the density n on the r.h.s. of Eq. (4) ensures that $\int dc \tilde{f}(c) = 1$ and $\int dc c^2 \tilde{f}(c) = d/2$. This scaling function describing the homogeneous cooling state satisfies the time-independent equation [2, 4, 8]

$$\frac{\mu_2}{d} \left(d + c_1 \frac{d}{dc_1} \right) \tilde{f}(c_1) = \tilde{I}(\tilde{f}, \tilde{f}), \quad (5)$$

where

$$\mu_p = - \int_{\mathbb{R}^d} d\mathbf{c}_1 c_1^p \tilde{I}(\tilde{f}, \tilde{f}), \quad (6)$$

and

$$\tilde{I}(\tilde{f}, \tilde{f}) = \int_{\mathbb{R}^d} d\mathbf{c}_2 \int d\hat{\boldsymbol{\sigma}} \theta(\hat{\boldsymbol{\sigma}} \cdot \hat{\mathbf{c}}_{12}) (\hat{\boldsymbol{\sigma}} \cdot \mathbf{c}_{12}) \left[\frac{1}{\alpha^2} f(c_1^{**}) f(c_2^{**}) - f(c_1) f(c_2) \right]. \quad (7)$$

It is useful to consider the hierarchy of moment equations obtained by integrating Eq. (5) over c_1 with weight c_1^p [4]

$$\mu_p = \frac{\mu_2}{d} p \langle c^p \rangle. \quad (8)$$

The solution of Eq. (5) is non-Gaussian in several respects. The high energy tail is overpopulated compared to the Maxwellian [4], a generic although not systematic feature for granular gases (a particular heating mechanism leading to an under-population at large velocities has been studied in [8]). Deviation from Gaussian behavior may also be observed at thermal scale or near the velocity origin. To study the latter correction, it is convenient to resort to a Sonine expansion for the distribution function $\tilde{f}(c)$ [19]

$$\tilde{f}(c) = \mathcal{M}(c) \left[1 + \sum_{i \geq 1} a_i S_i(c^2) \right], \quad (9)$$

where $\mathcal{M}(c) = \pi^{-d/2} \exp(-c^2)$ is the Maxwellian, and $S_i(c^2)$ the Sonine polynomials (that may be found in [19]; the first few are recalled in [4]). Due to the constraint $\langle c^2 \rangle = d/2$ the first correction a_1 vanishes [4], and for our purposes it is sufficient to know $S_2(x) = x^2/2 - (d+2)x/2 + d(d+2)/8$. From Eq. (9) and making use of the orthogonality of the Sonine polynomials with respect to a Gaussian measure, one may relate the coefficient a_2 to the kurtosis of the velocity distribution

$$\langle c^4 \rangle = \frac{d(d+2)}{4} (a_2 + 1), \quad (10)$$

so that, upon taking $p = 4$ in Eq. (8), we get

$$\mu_4 = (d+2)(1+a_2)\mu_2. \quad (11)$$

In the following analysis, we will only retain the first correction in the expansion (9): $\tilde{f} = \mathcal{M}(1 + a_2 S_2)$. Computing μ_2 and μ_4 to linear order in a_2 with this functional ansatz [and further linearizing Eq. (11)], one deduces a_2 [4, 8]. This approach is nonperturbative in the restitution coefficient. However, since the high energy tail of $\mathcal{M}(1 + a_2 S_2)$ is very distinct from that of the exact solution of Eq. (5), computing a_2 from relation (8) with $p > 4$ is expected to give a poor estimate, all the worse as p increases. With this in mind, it appears that the limit of vanishing velocity of the rescaled Boltzmann equation (5) contains an interesting piece of information:

$$\mu_2 \tilde{f}(0) = \lim_{c_1 \rightarrow 0} \tilde{I}(\tilde{f}, \tilde{f}). \quad (12)$$

The main steps to compute this limit are given in appendix. Up to a geometrical prefactor, the loss term of $\lim \tilde{I}$ on the r.h.s. reads $\tilde{f}(0) \langle c_1 \rangle$ and is thus of lower order than the quantities appearing in (11). Working at linear order in a_2 , one may therefore expect to achieve a better accuracy when computing the various terms (except may be the gain term) appearing in (12) than in (11). In the context of ballistic annihilation, a related remark lead to analytical predictions for the decay exponents of the dynamics and non-Gaussian features of the velocity statistics, in excellent agreement with the numerical simulations [15, 16]. In the present situation, the gain term of \tilde{I} in (12) cannot be written as a collisional moment, so that the situation is less clear and deserves some investigation. We propose to

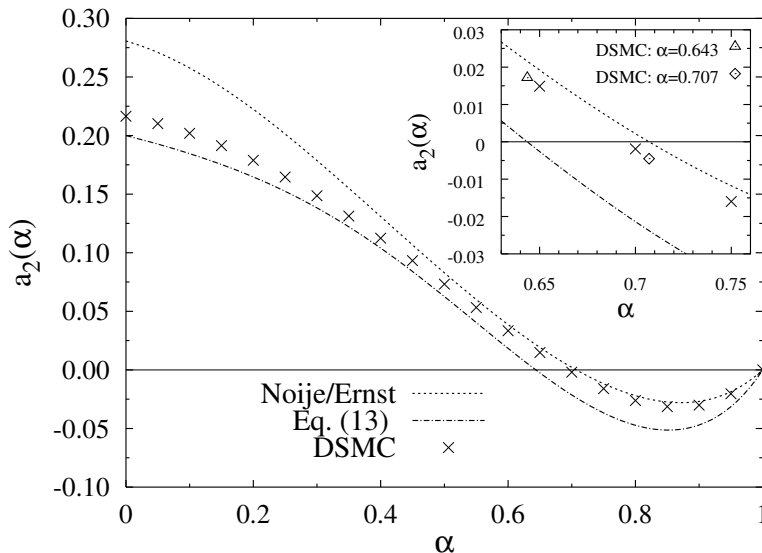


FIG. 1: Comparison of the correction $a_2(\alpha)$ for the free cooling in two dimensions obtained in [4], with Eq. (13). The crosses correspond to the “exact” result, obtained by solving the Boltzmann equation with the DSMC method, for 10^6 particles and approximately 500 collisions for each particle. The inset is a zoom in the region of the smallest root of the fourth cumulant.

compare the value of a_2 following this route to the standard one of Refs. [4, 8, 14]. Evaluating (12) at first order in a_2 , we obtain:

$$a_2 = \frac{4(\alpha^2 + 1)^2(\alpha^2 - 1) [\sqrt{2}(\alpha^2 + 1) - 2]}{A(\alpha, d)}. \quad (13)$$

where

$$A(\alpha, d) = 5 + d(2 - d) + 8\alpha(\alpha^2 + 1)(d - 1) - \alpha^2(23 - 6d + d^2) + \alpha^4(3 + 6d + d^2) + \alpha^6(-1 + 2d + d^2) - \sqrt{2}(\alpha^2 + 1)^3(\alpha^2 - 1)(3 + 4d + 2d^2)/4. \quad (14)$$

In Fig. 1, we compare this result with the analytical expression of van Noije and Ernst [4]. We also display the fourth cumulant a_2 obtained by Monte Carlo simulations from the numerical solution of the nonlinear Boltzmann equation (1) (so called DSMC technique [20, 21]). Our expression appears more accurate at small inelasticity, but less satisfying close to elastic behavior. The smallest root of $a_2 = 0$ obtained with Eq. (13) is $\alpha^* = (\sqrt{2} - 1)^{1/2} \simeq 0.643\dots$. This root differs from the value $\alpha^{**} = 1/\sqrt{2} \simeq 0.707\dots$ obtained upon solving (11) (both α^* and α^{**} do not depend on space dimension d). The inset shows that the exact root is located in the interval $]\alpha^*, \alpha^{**}[$, and seems closer to α^{**} .

In order to understand the discrepancy close to the elastic limit shown in Fig. 1, it is useful to study the first Sonine correction $\tilde{f}(c_i)/\mathcal{M}(c_i) = 1 + a_2 S_2(c_i^2)$. The result for $\alpha = 0.8$ where our method seems to be the less accurate is shown in Fig. 2, and in Fig. 3 for $\alpha = 0.5$.

In spite of the imprecision of our analytical expression for a_2 seen in Fig. 1, Fig. 2 shows that the limit method is very accurate for small velocities, but turns to quickly become more imprecise for bigger velocities. This suggests that computing the fourth cumulant from the limit of vanishing velocities gives more weight to this region which leads to a better behavior of the Sonine expansion for small velocities. On the other hand, the traditional route yields a global interpolation for all velocities. The good precision of our result for small velocities and the lower accuracy for higher velocities is confirmed in Fig. 3. Exploiting the above qualitative interpretation of the limit method, we expect to achieve a good accuracy using Eq. (13) in order to find the first moment [16]:

$$\langle |c| \rangle = \frac{\sqrt{\pi}}{2} \left(1 - \frac{a_2}{8} \right). \quad (15)$$

Indeed, we suppose that the function a_2 obtained from the limit method gives a precise description of the rescaled velocity distribution for small velocities. Thus our a_2 is likely to describe more accurately a low order velocity moment than a high order one. This is confirmed by Fig. 4.

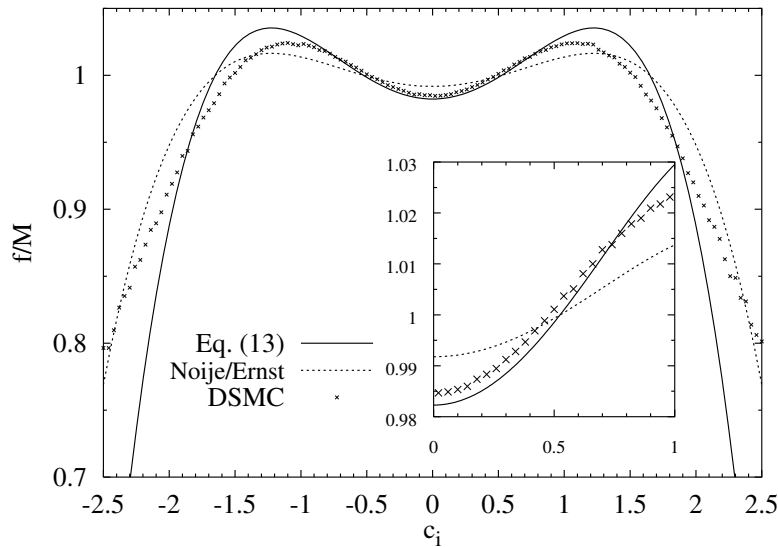


FIG. 2: Plot of $\tilde{f}(c_i)/\mathcal{M}(c_i)$ for $\alpha = 0.8$. The curve labelled “Eq. (13)” and “Noije/Ernst” correspond to $1 + a_2 S_2$ where a_2 is given respectively by Eq. (13) and by the Sonine correction obtained by Noije and Ernst following the traditional route [4]. “DSMC” refers to the full distribution obtained from the solution of the Boltzmann equation (using 10^6 particles and averaging over 300 independent samples).

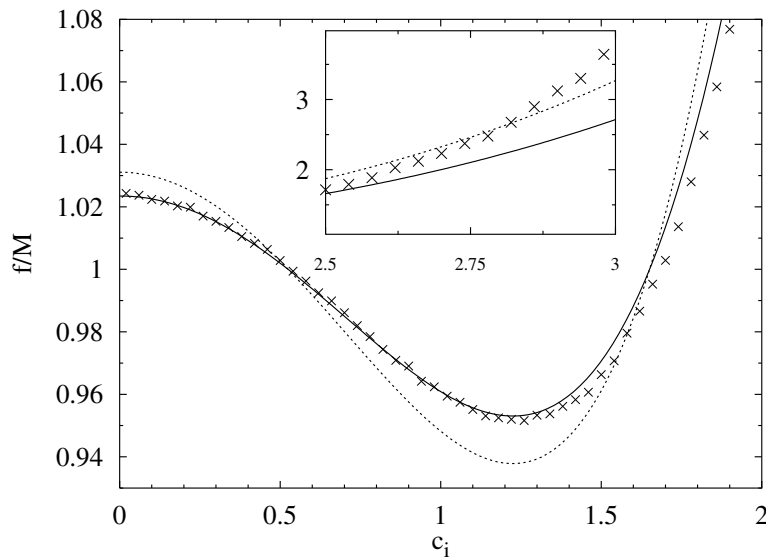


FIG. 3: Same as Fig. 2 for $\alpha = 0.5$.

As emphasized by Montanero and Santos [8], a certain degree of ambiguity is present when evaluating an identity such as (11) or (12) to first order in a_2 . According to the way we rearrange the terms μ_4 , μ_2 , and $(d+2)(1+a_2)$ in say Eq. (11) and subsequently apply a Taylor series expansion in a_2 , we obtain different predictions for $a_2(\alpha)$. For instance van Noije and Ernst did expand the relation (11) [4], whereas Montanero and Santos also considered other possibilities such as $\mu_4/\mu_2 = (d+2)(1+a_2)$ (this leads to a result which turns out to be fairly close to the one in [4]) and also $\mu_4/(1+a_2) = (d+2)\mu_2$. For small α in the latter case, the resulting a_2 turns out to be 20% lower than the previous ones, and very close to the exact (within Boltzmann’s equation framework) numerical results, for all the values of the restitution coefficient [8]. We push further this remark and show in Fig. 5 the eight simplest different possible functions $a_2(\alpha)$ obtained upon rearranging the terms of Eq. (11) and expanding the result to first

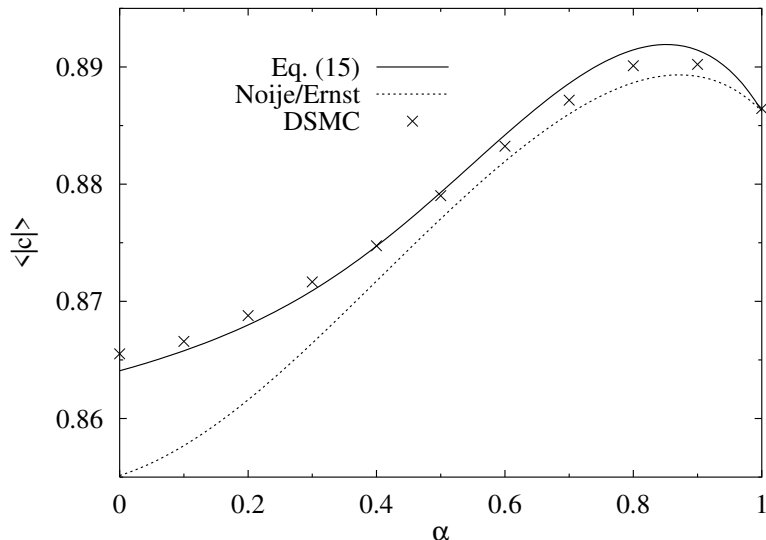


FIG. 4: First rescaled velocity moment $\langle |c| \rangle$ as a function of the restitution coefficient. DSMC is done for 10^5 particles and approximately 500 collisions for each particle.

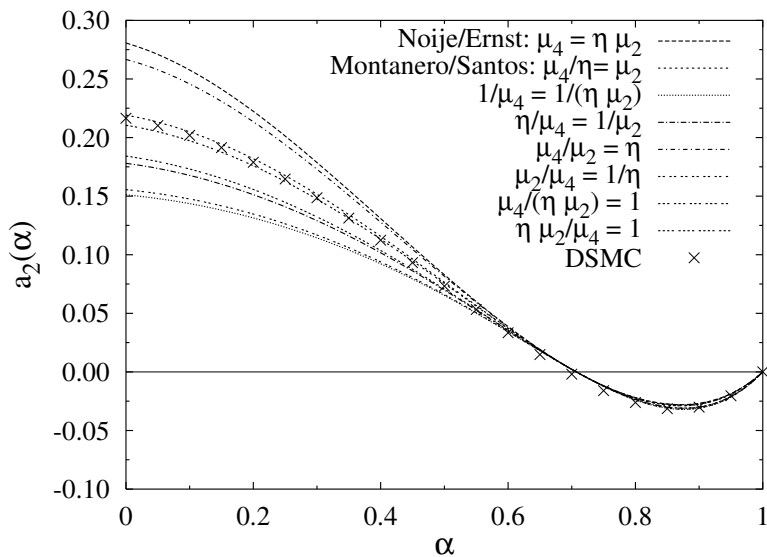


FIG. 5: The eight possible fourth cumulant a_2 obtained from Eq. (11), corresponding to the two-dimensional homogeneous free cooling. We define $\eta = (d+2)(1+a_2)$, then rewrite the equation $\mu_4 = \eta\mu_2$ according to the eight possible different combinations mentioned in the legend, before doing the linear Taylor expansion around $a_2 = 0$. The first curve is the plot of the function a_2 obtained by van Noije and Ernst [4], whereas the second one – obtained by Montanero and Santos [8] – is very close to the exact results shown by crosses.

order in a_2 . A similar ambiguity is present making use of Eq. (12). The corresponding eight different possibilities are plotted in Fig. 6. It appears that the envelope of the curves following from this method is less spread than within the “traditional” route, by a factor of approximately 2. We thus achieve a better accuracy at small α .

The dispersion of the curves in Figs. 5 and 6 illustrates the nonvalidity of the linearization approximation at small α . However –and concentrating on Fig. 5– it appears that all curves do not have the same status. Brilliantov and Pöschel have indeed solved analytically the full nonlinear problem [i.e. working again with the distribution function $\tilde{f} = \mathcal{M}(1 + a_2 S_2)$ but keeping nonlinear terms in a_2], and obtained results that are very close to those of Noije/Ernst,

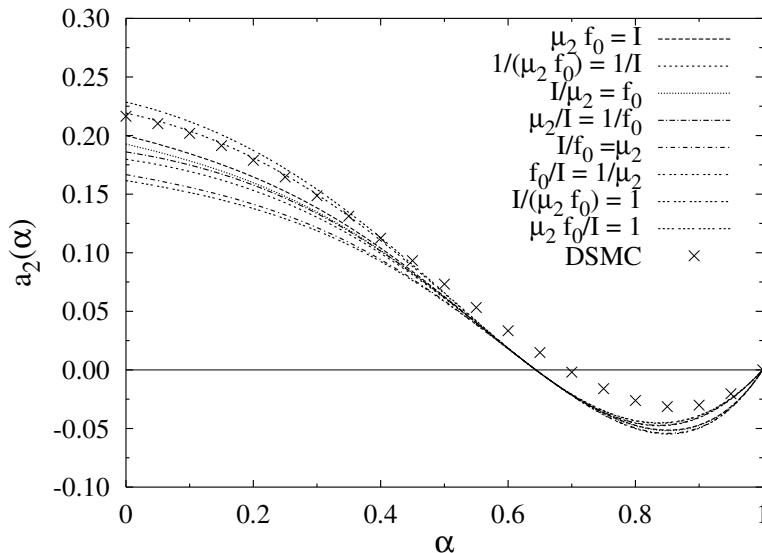


FIG. 6: Same as Fig. 5, making use of Eq. (12) instead of (11) to compute the first Sonine correction. In the legend, I denotes $\lim \tilde{I}$ and $f_0 = \tilde{f}(0)$.

except for $\alpha < 0.2$ where they found slightly larger fourth cumulants [9]. Their result is therefore farther away from the exact one obtained by DSMC (see e.g. Fig. 1 where it appears that the Noiye/Ernst expression already overestimates the exact curve). The difference between the DSMC results and those of Brilliantov/Pöschel therefore illustrates the relevance of Sonine terms a_i with $i \geq 3$ in expansion (9). However, some of the curves shown in Fig. 5 lie close to the exact one, which means that it is possible to correct the deficiencies of truncating \tilde{f} at second Sonine order by an ad-hoc linearizing scheme. The agreement obtained is nevertheless incidental, and the corresponding analytical expression should be considered as a semi-empirical interpolation supported by numerical simulations. One should thus emphasize that the right way to compute a_2 is to use its definition involving the fourth rescaled velocity cumulant of Eq. (10) because this relation is not sensitive to higher order Sonine terms, nor to nonlinearities, even if this route doesn't give the most accurate description in the small velocity domain (as seen from Figs. 2 and 3)

For completeness, we now briefly consider the stochastic thermostat situation [4, 6, 8, 13], where the counterpart of Eq. (5) reads

$$-\frac{\mu_2}{2d} \nabla_{c_1}^2 \tilde{f}(c_1) = \tilde{I}(\tilde{f}, \tilde{f}). \quad (16)$$

Considering again the limit $c_1 \rightarrow 0$ and retaining only the first correction in the expansion (9), we get

$$\frac{\mu_2}{2\pi^{d/2}} \left[2 + a_2 \frac{(d+2)(d+4)}{4} \right] = \lim_{c_1 \rightarrow 0} \tilde{I}(\tilde{f}, \tilde{f}). \quad (17)$$

Given that the r.h.s. is already known from the free cooling calculation, it is straightforward to extend the previous results to the present case. As before, there are 8 possible ways to extract a_2 from Eq. (17) working at linear order. The resulting expressions are displayed in Fig. 7. On the other hand, the moment method described in Refs. [4, 8] makes use of the identity $\mu_2(d+2) = \mu_4$, that is a direct consequence of Eq. (16). There are thus 4 possible rearrangements leading to the different cumulants shown in the inset of Fig. 7. For comparison, we have also implemented Monte Carlo simulations in the present heated situation (see the crosses in Fig. 7). It is difficult to compare the dispersion of the curves with both methods (8 possibilities versus 4), since our approach makes use of Eq. (17) which is of higher order in a_2 than $\mu_2(d+2) = \mu_4$, the starting point used in Refs. [4, 8]. Our method appears here less accurate than for the free cooling, with again an underestimation of a_2 at large α .

In order to get free from the ambiguities inherent to a linear computation in a_2 , we have also solved the full nonlinear problem. The computation becomes cumbersome, and since Brilliantov and Pöschel [9] have already initiated this route in 3D for the homogeneous free cooling (thereby providing the calculation of μ_2 and μ_4), we will turn our attention to the 3D situation. First and for the sake of comparison, we have repeated the nonlinear derivation of Ref. [9] for the stochastic thermostat. Second, we have computed the right-hand sides of Eqs. (12) and (17) without any

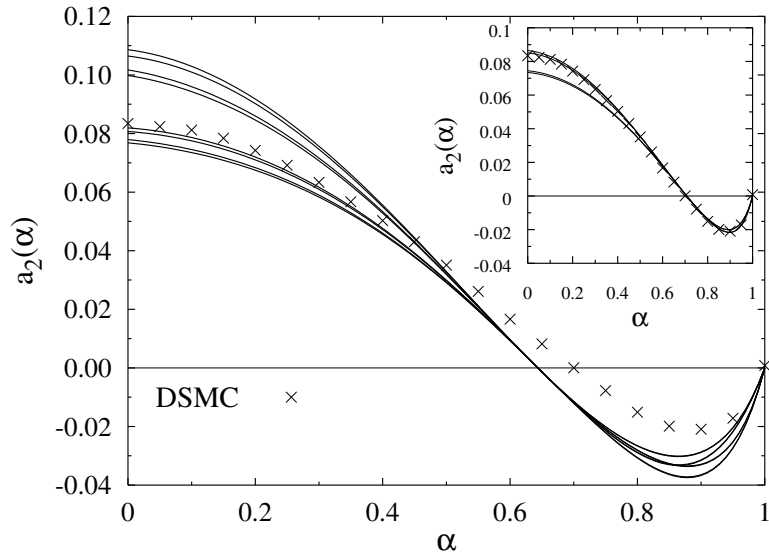


FIG. 7: The counterpart of Fig. 6 for the two dimensional stochastic thermostat. The inset shows the 4 possibilities associated with the method of Refs. [4, 8]. The symbols show the results of DSMC simulations.

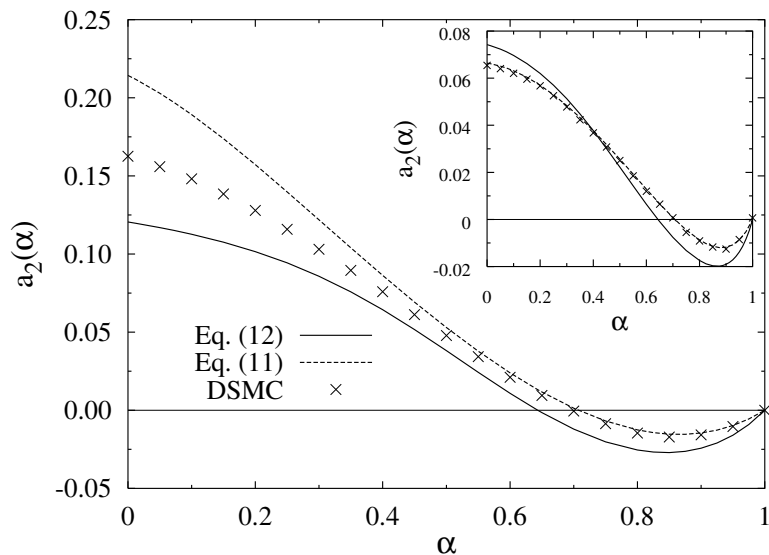


FIG. 8: Fourth cumulant in 3 dimensions for a force free system in the regime of homogeneous cooling. The curves correspond to the nonlinear solutions of Eqs. (11) and (12) (see text for details). The crosses correspond to the Monte Carlo results. The inset shows the same curves for the stochastic thermostat.

linearization, from the form $\tilde{f} = \mathcal{M}(1 + a_2 S_2)$. The left-hand sides only require the knowledge of μ_2 . For both free and forced situations, we subsequently obtain a polynomial equation of degree 3 for a_2 from which we extract the physical root, the two others corresponding to unstable scaling solutions [9]. The results are displayed in Fig. 8. In particular, our approach again suffers from an underestimation of a_2 for $\alpha > 0.5$, already observed within the linear computation, and that is thus ascribable to Sonine terms of order 3 or higher. In this respect, it is surprising that these terms do not affect similarly the moment method of Ref. [9] in the same range of inelasticities.

To sum up, using a new approach we obtain the first non-Gaussian correction a_2 to the scaled velocity distribution. In view of the above results, we conclude that our approach constitutes an improvement over the previous procedures in the small velocity regime, and our analysis turns to be technically simpler to perform. We have also discussed the

ambiguities that arise 1) when restricting ourselves to second Sonine order, and 2) when a further linearization of the various relevant relations is performed. It appears that an *ad-hoc* linearization scheme (point 2) may circumvent the limitations inherent to point 1. In any case, the computation of a non-Gaussian correction suffers from uncontrolled approximations that systematically need to be confronted against numerical simulations.

We acknowledge useful discussions with A. Santos and A. Barrat. This work was partially supported by the Swiss National Science Foundation and the French ‘‘Centre National de la Recherche Scientifique’’.

APPENDIX: CALCULATION OF THE LIMIT $c_1 \rightarrow 0$ OF THE COLLISION TERM

We define the loss term \tilde{I}_l and gain term \tilde{I}_g by

$$\tilde{I}_l = - \lim_{c_1 \rightarrow 0} \int_{\mathbb{R}^d} d\mathbf{c}_2 \int d\hat{\boldsymbol{\sigma}} \theta(\hat{\boldsymbol{\sigma}} \cdot \hat{\mathbf{c}}_{12})(\hat{\boldsymbol{\sigma}} \cdot \mathbf{c}_{12}) \tilde{f}(c_1) \tilde{f}(c_2) \quad (\text{A.1a})$$

$$\tilde{I}_g = \lim_{c_1 \rightarrow 0} \frac{1}{\alpha^2} \int_{\mathbb{R}^d} d\mathbf{c}_2 \int d\hat{\boldsymbol{\sigma}} \theta(\hat{\boldsymbol{\sigma}} \cdot \hat{\mathbf{c}}_{12})(\hat{\boldsymbol{\sigma}} \cdot \mathbf{c}_{12}) \tilde{f}(c_1^{**}) \tilde{f}(c_2^{**}), \quad (\text{A.1b})$$

so that $\lim_{c_1 \rightarrow 0} \tilde{I}(\tilde{f}, \tilde{f}) = \tilde{I}_l + \tilde{I}_g$.

Taking the limit $c_1 \rightarrow 0$ of the loss term yields the exact result

$$\tilde{I}_l = -\beta_1 \tilde{f}(0) \langle c_2 \rangle, \quad (\text{A.2})$$

where

$$\beta_1 = \int_{\mathbb{R}^d} d\hat{\boldsymbol{\sigma}} \theta(\hat{\boldsymbol{\sigma}} \cdot \hat{\mathbf{c}}_2)(\hat{\boldsymbol{\sigma}} \cdot \hat{\mathbf{c}}_2) = \frac{\pi^{(d-1)/2}}{\Gamma[(d+1)/2]}, \quad (\text{A.3})$$

with Γ the gamma function. Within the framework of the Sonine expansion (9), neglecting the coefficients a_i , $i \geq 3$, and making use of [16]

$$\langle c_2 \rangle = \left(1 - \frac{a_2}{8}\right) \frac{\Gamma[(d+1)/2]}{\Gamma(d/2)}, \quad (\text{A.4})$$

Eq. (A.2) becomes

$$\tilde{I}_l = -\frac{S_d \mathcal{M}(0)}{2\sqrt{\pi}} \left[1 + a_2 \frac{d(d+2)}{8}\right] \left(1 - \frac{a_2}{8}\right), \quad (\text{A.5})$$

where $S_d = 2\pi^{d/2}/\Gamma(d/2)$ is the surface of the d -dimensional sphere.

Defining $\beta = (1 + \alpha)/(2\alpha) > 1$, the precollisional rescaled velocities \mathbf{c}_i^{**} and postcollisional ones \mathbf{c}_i are related by

$$\mathbf{c}_1^{**} = \mathbf{c}_1 - \beta(\mathbf{c}_{12} \cdot \hat{\boldsymbol{\sigma}}) \hat{\boldsymbol{\sigma}}, \quad (\text{A.6a})$$

$$\mathbf{c}_2^{**} = \mathbf{c}_2 + \beta(\mathbf{c}_{12} \cdot \hat{\boldsymbol{\sigma}}) \hat{\boldsymbol{\sigma}}. \quad (\text{A.6b})$$

The gain term (A.1b) thus becomes

$$\tilde{I}_g = \frac{1}{\alpha^2} \int_{\mathbb{R}^d} d\mathbf{c}_2 \int d\hat{\boldsymbol{\sigma}} \theta(\hat{\boldsymbol{\sigma}} \cdot \hat{\mathbf{c}}_2)(\hat{\boldsymbol{\sigma}} \cdot \mathbf{c}_2) \tilde{f}[\beta(\mathbf{c}_2 \cdot \hat{\boldsymbol{\sigma}}) \hat{\boldsymbol{\sigma}}] \tilde{f}[\mathbf{c}_2 - \beta(\mathbf{c}_2 \cdot \hat{\boldsymbol{\sigma}}) \hat{\boldsymbol{\sigma}}], \quad (\text{A.7})$$

where the function \tilde{f} is isotropic. Performing the integration over \mathbf{c}_2 before that over $\hat{\boldsymbol{\sigma}}$, we choose the x Cartesian coordinate as corresponding to the $\hat{\boldsymbol{\sigma}}$ direction. The velocity \mathbf{c}_2 is thus written $\mathbf{c}_2 = c_x \hat{\mathbf{x}} + \mathbf{c}_\perp$, with $c_x = (\mathbf{c}_2 \cdot \hat{\boldsymbol{\sigma}}) \in \mathbb{R}$ and $\mathbf{c}_\perp = \mathbf{c}_2 - c_x \hat{\mathbf{x}} \in \mathbb{R}^{d-1}$. Eq. (A.7) becomes

$$\tilde{I}_g = \frac{1}{\alpha^2} \int d\hat{\boldsymbol{\sigma}} \int_{\mathbb{R}^d} d\mathbf{c}_2 \theta(c_x) c_x \tilde{f}(\beta c_x \hat{\boldsymbol{\sigma}}) \tilde{f}(\mathbf{c}_2 - \beta c_x \hat{\boldsymbol{\sigma}}) \quad (\text{A.8})$$

$$= \frac{S_d}{\alpha^2} \int_0^\infty dc_x c_x \int_{\mathbb{R}^{d-1}} d\mathbf{c}_\perp \tilde{f}(\beta c_x) \tilde{f}\left(\sqrt{c_\perp^2 + c_x^2(1-\beta)^2}\right). \quad (\text{A.9})$$

Eq. (A.9) is an exact relation within Boltzmann's framework. Making use of the the Sonine expansion (9) where we retain only the first correction a_2 , Eq. (A.9) becomes

$$\tilde{I}_g = \frac{S_d}{\alpha^2 \pi^d} \int_0^\infty dc_x c_x e^{-[\beta^2 + (1-\beta^2)]c_x^2} \int_{\mathbb{R}^{d-1}} d\mathbf{c}_\perp e^{-c_\perp^2} [1 + a_2 S_2(\beta^2 c_x^2)] \{1 + a_2 S_2 [c_\perp^2 + c_x^2(1-\beta)^2]\}. \quad (\text{A.10})$$

With the definition of the second Sonine polynomial $S_2(x) = x^2/2 - (d+2)x/2 + d(d+2)/8$, one sees that Eq. (A.10) may be expressed as a sum of products of the integrals

$$J_\perp(n) = \int_{\mathbb{R}^{d-1}} d\mathbf{c}_\perp e^{-c_\perp^2} c_\perp^n, \quad (\text{A.11a})$$

$$J_x(n) = \int_0^\infty dc_x e^{-[\beta^2 + (1-\beta^2)]c_x^2} c_x^n, \quad (\text{A.11b})$$

that may be computed using the general relation ($a > 0$)

$$\int_{\mathbb{R}^d} d\mathbf{x} |\mathbf{x}|^n e^{-a\mathbf{x}^2} = \frac{\pi^{d/2}}{a^{(d+n)/2}} \frac{\Gamma[(d+n)/2]}{\Gamma(d/2)}. \quad (\text{A.12})$$

Tedious but technically simple calculations thus lead to

$$\tilde{I}_g = \frac{S_d \mathcal{M}(0)}{2\sqrt{\pi}} \left[\frac{2}{1+\alpha^2} + a_2 D_1(\alpha, d) + a_2^2 D_2(\alpha, d) \right], \quad (\text{A.13})$$

where the final expressions $D_1(\alpha, d)$ and $D_2(\alpha, d)$ are too cumbersome to be given here. Finally, the limit $c_1 \rightarrow 0$ of Eq. (7) is given by the sums of Eqs. (A.5) and (A.13).

-
- [1] S. McNamara and W.R. Young, *Phys. Fluids A* **5**, 34 (1993).
 - [2] J.J. Brey, M.J. Ruiz-Montero, and D. Cubero, *Phys. Rev. E* **54**, 3664 (1996).
 - [3] N. Sela and I. Goldhirsch, *J. Fluid Mech.* **361**, 41 (1998).
 - [4] T.P.C. van Noije and M.H. Ernst, *Granular Matter* **1**, 57 (1998) (e-print: cond-mat/9803042).
 - [5] J.J. Brey, J.W. Dufty, C.S. Kim, and A. Santos, *Phys. Rev. E* **58**, 4638 (1998).
 - [6] T.P.C. van Noije, M.H. Ernst, E. Trizac, and I. Pagonabarraga, *Phys. Rev. E* **59**, 4326 (1999).
 - [7] V. Garzó and J. Dufty, *Phys. Rev. E* **60**, 5706 (1999).
 - [8] J.M. Montanero and A. Santos, *Granular Matter* **2**, 53 (2000) (e-print: cond-mat/0002323).
 - [9] N.V. Brilliantov and T. Pöschel, *Phys. Rev. E* **61**, 2809 (2000).
 - [10] R. Caferio, S. Luding, and H.J. Herrmann, *Phys. Rev. Lett.* **84**, 6014 (2000).
 - [11] R. Soto and M. Maréchal, *Phys. Rev. E* **63**, 041303 (2001).
 - [12] A. Barrat and E. Trizac, *Phys. Rev. E* **66**, 051303 (2002).
 - [13] A. Barrat, T. Biben, Z. Rácz, E. Trizac, and F. van Wijland, *J. Phys. A* **35**, 463 (2002) (e-print: cond-mat/0110345).
 - [14] A. Barrat, E. Trizac, and J.N. Fuchs, *Eur. Phys. J. E* **5**, 161 (2001).
 - [15] E. Trizac, *Phys. Rev. Lett.* **88**, 160601 (2002).
 - [16] J. Piasecki, E. Trizac, and M. Droz, *Phys. Rev. E* **66**, 066111 (2002).
 - [17] E. Ben-Naim, S. Redner, and F. Leyvraz, *Phys. Rev. Lett.* **70**, 1890 (1993).
 - [18] P.L. Krapivsky and C. Sire, *Phys. Rev. Lett.* **86**, 2494 (2001).
 - [19] L. Landau and E. Lifshitz, *Physical Kinetics*, Pergamon Press (1981).
 - [20] G. Bird *Molecular Gas Dynamics and the Direct Simulation of Gas Flows*, Clarendon Press, Oxford, (1994).
 - [21] J.M. Montanero, V. Garzó, A. Santos, and J.J. Brey, *J. Fluid Mech.* **389**, 391 (1999).